AGARD-AG-195 Evaluation of the potential benefit to the aeronautical field from laser technology

CHAPTER 10

OPTICAL CORRELATION

by

J.A.Boden
Physics Laboratory NDRO-TNO
The Hague – The Netherlands

CONTENTS

SUMMARY

A survey is given of the most common types of coherent optical correlators, which are classified as spatial plane correlators, frequency plane correlators and special reference correlators. Only the spatial plane correlators are dealt with rather thoroughly. Basic principles, some special features, advantages and disadvantages mostly are given with references to relevant literature.

Optical processing of sideways looking synthetic aperture radar data and the acousto-optical processing of linear FM radar signals are described (rather shortly) as special reference correlators, of which the first has become the most important application of optical data processing to date.

Some advantages and disadvantages of incoherent correlators are given for comparison along with some examples of the most common types. A detailed description of a simple coherent spatial plane correlator is given. Some experimental results are mentioned. The reference function in this correlator is realized as a hard clipped phase plate, which results in a large detection region and a high signal output; only one transforming lens is needed. The experimental results were fully in agreement with the calculated and/or expected values (only non real-time photographic film signal input was investigated).

Principles and the use as real-time input devices of ultrasonic light modulators are shortly reviewed.

A short description is given ~~for~~ of some erasable and reusable film types of which some relevant parameters for real-time operation are listed in a table.

1. INTRODUCTION

Optical correlation is a special branch of optical data processing and is mainly concerned with the computation of a correlation integral. Such an operation can often be performed in a coherent optical system because of the property that Fourier transform relations exist between the light amplitude distribution at the front and back focal plane of a lens[1-5]

If (see Figure 1) an amplitude transmission function $s(x)$ in the x-plane is illuminated by a plane wave $A\exp(j\omega t)$ then the amplitude distribution in the u-plane, which is the back focal plane of lens L1, will be

$$g(u) = \int A\, s(x) \exp\{-2\pi j(u/\lambda F)x\}dx . \qquad (1.1)$$

Here λ is the wavelength of the light and F the focal length of the lens.

With another lens, as is given in Figure 1 by lens L2, the amplitude distribution in the x′-plane, which is the back focal plane of lens L2, will then be:

$$s'(x') = \int g(u) \exp\{-2\pi j(x'/\lambda F)u\}du = As(-x') . \qquad (1.2)$$

So the x-plane is imaged onto the x′-plane.

The configuration in Figure 1 is the basic one of any optical data processing system. Depending on the application a short system with one lens or a longer one with two or more lenses is applied.

Most applications of coherent optical systems make use of the fact that in such a system the spatial frequencies of the input function(s) are physically separated in the frequency planes.

Operations can be performed on the amplitudes and/or phases of the light distributions in the object planes (hereafter called spatial planes) or in the frequency planes.

This can be done by adding fixed or varying transmission masks in the relevant planes. Also studies can be made of the spatial frequency distribution of input functions.

The main applications of optical processing methods will be found in

(a) spectrum analysis,

(b) frequency plane (matched) filtering,

(c) (multi channel) correlation.

The power of the optical system lies in its two-dimensional nature, which permits either the processing of two-dimensional signals or the simultaneous processing of a large number of one-dimensional signals; the latter can be accomplished by the use of cylindrical optics.

Only in areas where vast numbers of calculations (linear operations) must be performed per unit time optical systems can compete with e.q. digital computers. The latter have a better accuracy and can perform more complex operations but they have a far lower speed[5,6,8,9,10].

Therefore the major applications of coherent optical computing to date have become: coherent side-looking synthetic-aperture radar signal processing, optical image deblurring and pattern recognition[6].

There is an enormous amount of good literature (also review literature) on optical data processing techniques and applications; therefore in this paper often will be referred to books and review articles which contain many important references.

Fundamental aspects can be found in References 2 – 5.

Preston's book[5] is the most recent review of all the separate aspects of optical computing with many references.

Felstead's report[11] shortly reviews optical correlation methods with a lot of references; the report itself is mainly concerned with "pseudo-coherent" optical correlation techniques.

Stroke[6] and Preston[5] give a number of the most important industrial and academic research laboratories where important work on optical computing has been done and/or is going on.

2. COHERENT OPTICAL CORRELATORS

2.1 Spatial Plane Correlators

2.1.1 Squared Correlation Function

Optical correlators mostly are concerned with the computation of the correlation integral

$$R_{12}(\tau) = \int s_1(x)\, s_2(x + \tau)\, dx \,. \tag{2.1}$$

Here x is a spatial coordinate and τ the relative delay between the two signals.

A linear operation as Equation (2.1) frequently must be performed in e.g. radar and sonar pulse-compression systems (in an appropriate pulse compression system a resolution improvement equal to the time-bandwidth product TW of the signal can be obtained theoretically). The correlation integral $R_{12}(\tau)$ can easily be found in a frequency-plane of a coherent optical system (see Figure 1).

The amplitude as well as the phase of the light distribution contains information about the input functions; the phase information is preserved only if coherent detection is applied[23,26], but mostly intensity detection is performed and then the squared correlation function $|R_{12}(\tau)|^2$ will be measured[12-19].

A correlator is called a spatial plane correlator[11-27] if both functions $s_1(x)$ and $s_2(x)$ are situated in a spatial plane; either they are put side by side in one plane (e.g. the x-plane in Figure 1) or one of the functions is imaged onto the other (e.g. $s_1(x)$ in the x-plane and $s_2(x)$ in the x'-plane, Figure 1).

In the latter case some prefiltering can be performed on the first function; in the first case correlators with only one transforming lens can be built, which have the additional advantage that imaging problems are reduced and the mechanical stability is increased.

Suppose a fixed amplitude transmission function $s_1(x)$ is in the x-plane of Figure 1 and an amplitude transmission function $s_2(x)$ is moving along $s_1(x)$ in the same plane. If these functions are illuminated by a plane wave: $A \exp(j\omega t)$, an amplitude distribution in the u-plane (back focal plane of lens L1) will be found:

$$g(u, \tau) = A\, e^{j\omega t} C_0 \int s_1(x) s_2(x + \tau)\, e^{-2\pi j(u/\lambda F)x} dx \,. \tag{2.2}$$

So in $u = 0$ the result is:

$$g(o, \tau) = A\, e^{j\omega t}\, C_0 \int s_1(x)\, s_2(x + \tau)\, dx = C_1 \cdot R_{12}(\tau) \tag{2.3}$$

which is the correlation function of $s_1(x)$ and $s_2(x)$.

At the same time can be detected in $u = u_0 \neq 0$ the correlation function of $s_2(x)$ and $s_1(x) \exp\{-2\pi j(u_0/\lambda F)x\}$.

The latter can be seen as a frequency shifted version of $s_1(x)$: thus with one reference function $s_1(x)$ the correlation-functions of all possible frequency shifted versions of $s_1(x)$ with the input signal $s_2(x)$ can simultaneously be generated. This feature becomes very attractive if the input functions are modulated carrier waves: the signal's delay and its frequency shift can simultaneously be measured[12-14].

A detailed description of such a correlator will be given in Section 4.

The second spatial dimension can still be used to perform multichannel operation.

2.1.2 D–c Bias Level

Functions of which a correlation integral must be obtained mostly are time functions, which have to be recorded as spatial amplitude or phase transmission functions.

This can be done on photographic transparancies but then a d–c bias level has to be added in order to register negative values too. The transmission functions then become

$$T_1(x) = a_1 + b_1\, s_1(x) \tag{2.4}$$

$$T_2(x + \tau) = a_2 + b_2\, s_2(x + \tau) \tag{2.5}$$

and the amplitude distribution in the u-plane:

$$g(u, \tau) = C_1 \int \{a_1a_2 + a_2b_1s_1(x) + a_1b_2s_2(x + \tau) + b_1b_2s_1(x)s_2(x + \tau)\}\, e^{-2\pi j/\lambda F.ux}\, dx \,. \qquad (2.6)$$

The bias term a_1a_2 now represents a wave travelling parallel to the optical axis and especially this term will prevent correlation detection around $u = 0$ in the frequency plane.

Many correlators differ only in the method of d–c bias removal; this will depend sometimes on the kind of signal and signal display, that is applied. One major form of bias removal consists in putting an optical stop in the frequency plane at $u = 0$ (Refs 5, 15, 17, 26).

The function whose zero-order has to be removed, is put in the x-plane and imaged onto the second function in the x′-plane (Fig.1); the correlation integral then can be found in the u′-plane.

Besides the fact that more lenses of good quality are needed, this long system will give rise to alignment and mechanical stability problems.

An interesting form is the folded system of Izzo[17], who used the same Fourier-transform lens three times by the utilisation of a reflective spatial-frequency-plane filter (in the u-plane, Figure 1). Another method can be found in compensating the zero order by a weighted plane wave, that is shifted over π radians in a Mach-Zehnder interferometer[29,30]: optical path length fluctuations however then become an important source of noise. A better solution to the problem is the use of carrier waves, which leads to off-axis correlation detection; an inherent advantage then is the possibility of frequency shift detection on the same frequency axis[12–15,28].

Felstead[14] uses in his off-set frequency method different carrier frequencies for the two signals: the transmission functions then become:

$$T_1(x) = a_1 + b_1 s_1(x) \cos\{(\omega_c + \Delta\omega)x + \alpha_1(x)\} \,. \qquad (2.7)$$

$$T_2(x + \tau) = a_2 + b_2 s_2(x + \tau) \cos\{\omega_c(x + \tau) + \alpha_2(x + \tau)\} \,. \qquad (2.8)$$

This leads to 9 spectral terms in the frequency plane.

A certain region around the difference frequency $\Delta\omega$, where the correlation occurs, is free from spurious terms.

In such a correlator 1/256 part of the input power can be focussed in each correlation peak under optimum conditions. Yet a more simple and efficient form can be acquired if a hard clipped phase function, with essentially no zero order, is used as reference function[12,13].

In the case of a phase transmission function and a photographic transparancy[13] e.g. only 3 terms will be generated in the frequency plane: two correlation terms and one spectral term around $u = 0$, without a zero order peak (see Section 4, Figure 3). In this case 1/16 part of the input power can be focussed in each correlation peak.

In most optical correlators use is made of one or more Ultrasonic Light Modulators (ULM) as input devices, which makes them appropriate for radar signal processing (see Section 5.1) Refs 11–12, 15–28. Besides the higher frequency processing capability especially the real-time operation capability is very attractive; as disadvantages should be mentioned the limited multi-channel operation and the lack of information storage capacity. Most of the ULM devices in the given references work in the Raman-Nath mode; some in the Bragg mode, which lead to higher output signals but which have generally lower coding flexibility (e.g. in References 12, 18, 19, 28).

In the Raman-Nath mode the maximum phase excursion in general will not be larger than 0.1 radians; the generated spatial phase-modulated transmission mask then acts somewhat like a amplitude transmission mask.

Suppose a signal $s(t) = a(t) \cos \omega_0 t$ is applied to the piezo-electric transducer of a ULM. Then the transmission can be given by:

$$T(x, \tau) = \exp\{jCa(x - vt) \cos \omega_c(x - vt)\} = \{1 + jCa(x - vt) \cos \omega_c(x - vt)\} \,. \qquad (2.9)$$

Here v = the velocity of the sonic wave and $\tau = vt$ is the delay. Thus here also a large d–c level is present that sometimes must be filtered. The j-factor implies a $\pi/2$ rad. phase shift between the modulated and the unmodulated light, which becomes important in some linear optical correlators[11,19].

If flexible coding is desired another ULM device for the reference function can be applied[16–19,28]; in general this will lower the output signal intensity.

2.1.3 *Linear Correlation Function*

Instead of measuring the squared correlation function $|R_{12}(\tau)|^2$ it is also possible to measure the linear correlation function $R_{12}(\tau)$ (Refs 5, 11, 19–27, 29).

This can be done by coherent detection in the frequency-plane[27], by integration over a time interval[29] or by integration over a spatial interval which mostly is performed on the photo-detector surface[5,11,19–26].

Carrier waves are required for this latter type of correlation.

Let the transmission functions in the input plane be:

$$T_1(x) = a_1 + b_1 s_1(x) \cos\{\omega_c x + \alpha_1(x)\} . \tag{2.10}$$

$$T_2(x+\tau) = a_2 + b_2 s_2(x + \tau) \cos\{\omega_c(x + \tau) + \alpha_2(x + \tau)\} . \tag{2.11}$$

Then the intensity distribution in the frequency-plane will be the squared Fourier-transform:

$$I(u, \tau) = |g(u, \tau)|^2 = \left| \int_{-\infty}^{+\infty} T_1(x) T_2(x + \tau) e^{-2\pi j/(u/\lambda F)x} \, dx \right|^2 . \tag{2.12}$$

Spatial integration on a photo-detector surface over that part of the u-plane, where e.g. one of the first diffraction orders is expected, will give an output:

$$v(\tau) = C \int_{u_1}^{u_2} |g(u, \tau)|^2 du \tag{2.13}$$

which will contain a component[11]:

$$V_1(\tau) = C' R_{12}(\tau) \cos\{\omega_c \tau + \phi(\tau)\} . \tag{2.14}$$

By bandpass filtering and envelope detecting the linear correlation function $R_{12}(\tau)$ can be determined. Most correlators in this class use a ULM as input device and a transmission replica as a reference function[11,19–20,23–26].

The spatial integration need not be performed in the frequency-plane, provided there is no overlap of the diffraction orders.

Sometimes the photodetector is placed directly after the transmission functions without the use of a lens; in that case some prefiltering must be performed[18] or the distance between the ULM and the reference mask must be accurately controlled[21–24].

Felstead[11] has shown that only a limited spatial coherence is needed for this class of correlators, which can therefore also be realized as "pseudo-coherent" correlators using an incoherent light source (see also Section 3.2: incoherent correlators).

A disadvantage of the linear correlator is the loss of frequency shift detection at the same time on the same frequency axis.

The homodyne correlator[5] is a special form of a linear optical correlator: spatial integration is performed over the squared sum of the separate spectra of the input functions.

The author is not aware of the existence of commercially available systems of spatial plane correlators, but they can easily be assembled. ULM devices can be supplied by several firms, however most of them work in the Bragg mode; the center frequencies used are below 150 MHz.

Most of the devices in the cited references use center frequencies below 50 MHz.

2.2 Frequency-Plane Correlators

In frequency-plane correlators the signal mask is put in a spatial plane (e.g. x-plane, Figure 1) and the reference mask in a frequency plane (e.g. u-plane, Figure 1). Mostly they are called matched-filter correlators.

The transmission of the reference-mask (the complex spatial filter) in the frequency-plane contains a term, which is proportional to the complex conjugate of the Fourier transform of the signal of which correlation detection is wanted.

If for example the input signal in the x-plane is $s(x)$ then the amplitude distribution in the u-plane will be:

$$g(u) = A_0 C \int_{-\infty}^{+\infty} s(x)\, e^{-2\pi j(u/\lambda F)x}\, dx \tag{2.15}$$

and if the transmission of the filter in the u-plane is proportional to:

$$g^*(u) = C' \int_{-\infty}^{+\infty} s^*(x) e^{2\pi j(u/\lambda F)x}\, dx \tag{2.16}$$

then the amplitude distribution in the x'-plane will contain:

$$s'(x') = C \int_{-\infty}^{+\infty} g(u)\, g^*(u) e^{-2\pi j(x'/\lambda F)u}\, du = A_0 C'' \int_{-\infty}^{+\infty} s(x) s^*(x + x')\, dx \tag{2.17}$$

which is the auto-correlation function of the input-signal.

The required filters generally are constructed by holographic methods[31,32]; computer generated filters also are used.

Applications can be found in pattern recognition[32] where the inherent two-dimensional capability of an optical system is essential. Cloud motion analysis may be mentioned as a typical example[38]. Multi channel frequency-plane matched filtering of one-dimensional signals in an astigmatic optical system is also possible[5].

Unfortunately the alignment and stability criteria are quite severe in matched filter correlation; especially during filter fabrication high-stability, both thermal and mechanical, is required, The filter re-positioning is sometimes quite critical[33,34].

Weaver et al.[33] overcome these positioning requirements by generating a photographic transparancy for each convolution that must be performed. Generating the filter in situ in real time can be advantageous. For that purpose photoplastic film can be a suitable material[38]. Also thermoplastic films[39] and photopolymers[38] will be of interest for real-time generation.

2.3 Special Reference Correlators

2.3.1 Synthetic Aperture Radar Signal Processing

The optical processing of synthetic aperture radar data has become the most important application of optical correlation to radar signal processing to date[7,35-37].

In this processing technique no reference transparancy is used, because the correlation is performed by the (*anamorphic*) lens system, that acts as a reference function itself.

In the side-looking synthetic-aperture radar technique short microwave frequency pulses are emitted in a slant range perpendicular to the flight direction. For each emitted pulse many back-scattered pulses are received, which will arrive at a time dependent on the range of the scatterer; the phase and amplitude of the composite signal are recorded by heterodyning the signal with a local oscillator. The incoming signal modulates the beam intensity of a cathode ray-tube, that is swept in the y-direction once for any transmitted pulse; a film moving in the x-direction and synchronized with the aircraft velocity records the CRT screen pattern: so the synthetic-aperture radar data are recorded as a two-dimensional pattern, of which the y-direction represents a slant range and the x-direction represents the along-track dimension. Each scatterer on the ground is represented as a one-dimensional Fresnel zone-plate on the film. This film is illuminated by a plane wave in an optical processor. Another film moves synchronically behind a slit in the plane where the Fresnel-zone plates are focussed by the use of an anamorphic lens system, thus at once generating a fine-resolution two-dimensional radar image from the raw radar data.

The amount of information received in a synthetic aperture system is so enormous that optical processing seems to be the most attractive one.

Especially at the University of Michigan important work in this field has been done (and is probably going on); their precision optical processor (POP) is probably the most sophisticated coherent optical computer; it has an equivalent digital processing rate of about 10^{12} bits per second and its original price is estimated to be about 250.000 dollars[9]. A microwave hologram system[7,37] in which synthetic aperture beam compression and phased array beam forming are accomplished simultaneously has also been examined and experimentally tested at the University of Michigan; furthermore this hologram radar is capable of generating range contours on terrain images in using a two-frequency interference technique. The field of view of this radar is directly below and to either side of the aircraft and is similar to that of airborne infrared and photographic systems.

2.3.2 *Linear FM Radar Signal Processing*

Another example of correlation, that needs no reference transparancy (and even no lens) can be found in the acousto-optical pulse compression of a linear FM modulated radar signal[19,28]. An accurately defined optical wavefront to perform the pulse compression acts here as the reference function.

If a linear FM signal is translated in a linear varying spatial phase modulated pattern by the use of a ULM device and this pattern is properly illuminated by a spherical wavefront there will be an instant for which the Bragg diffraction condition is satisfied simultaneously for all the frequencies in the generated phase pattern. At this instant the beam will be focussed to a single point without the use of lenses. The device will have a high signal output, but has only an impulse response for one type of signal; so the common flexibility of ULM devices is lost here.

3. INCOHERENT OPTICAL CORRELATORS

3.1 Characteristic Properties

For comparison some features of incoherent systems are mentioned here because often the light source could be replaced with advantage by a laser.

Characteristic properties of incoherent correlators are:

A. Neither point source nor single frequency illumination is needed.

B. If spatial frequencies are displayed the resolution is far beyond that of coherent systems.

C. Integration over the time and/or spatial dimension mostly is needed to get the required correlation function.

Owing to these characteristics, some advantages arise:

Due to A: Conventional light sources can be used.

Due to B and C: Relative wide apertures can be applied in the output plane, so the alignment, imaging and vibration problems are greatly reduced and a simple inexpensive optical system can be applied.

However, also important disadvantages arise:

Due to B: Less parameters can be measured simultaneously, so the processing capacity is substantially lowered in comparison with coherent systems.

Due to B: Requirements on frequency-plane filtering and d—c bias removal in general cannot be satisfied. The extraneous terms and/or the background illumination which cannot be removed from the output, now will lower the SNR and the dynamic range[5,11,42].

Due to B and C: A more complicated set up sometimes will be required to get the correlation function.

If in an incoherent system the light source is replaced by a laser but the same correlation detection method is applied in general the advantages will be maintained, some disadvantages will be overcome (the SNR will easily be improved in many cases) and new advantages will arise (e.g. sophisticated techniques such as electro-optical and acousto-optical modulation can be applied). The mentioned cost advantage of conventional light sources is relatively unimportant since HeNe lasers are available up from a hundred dollars.

3.2 Types of Incoherent Correlators

Roughly three types can be distinguished:

(*a*) CRT signal input

The input signal modulates the intensity of the CRT electron beam forming a pattern on the CRT screen. This pattern is cross-correlated by means of a set of reference transparancies contained in a reference mask that is located in front of the CRT screen. The transmitted light is focussed on the output device, that integrates the light until the entire correlation has been completed. Due to the d—c levels a large d—c background illumination can prevent correlation detection[40].

(*b*) Light source signal input

The incoming signal modulates the intensity of an incoherent light source and this light is collimated on a moving reference reticle. Mostly, behind this reticle an array of photodetectors (or image tube) is

placed, of which each element calculates by time integration a discrete value of the correlation function. Examples are found in sonar[41] as well as in radar signal processors[42-44].

Parks[41] uses the horizontal dimension of the reference mask for the coarse range resolution and the vertical dimension for the fine range resolution. The correlation function is generated in the vertical direction.

Skenderoff[42] uses the horizontal dimension for range and the vertical dimension for range-rate detection. His reference mask contains 20 different doppler replicas in the vertical direction. In each different doppler channel 600 ranges can be resolved.

The correlation function is generated in the horizontal dimension. Talamini[44] describes an analogous system, in which 1,200 range elements x 240 doppler elements = 288,000 range-doppler elements can be read out.

(*c*) Transmission mask signal input

The input signal is recorded as a spatial varying transmission function (either by applying the signal to an ULM device or by recording it on a moving film) and this function then moves along the reference function. The transmitted portion of a collimated beam of incoherent light mostly is integrated by a photodetector surface to perform the correlation function. To this class also belong the linear optical correlators, which are described as pseudo-coherent correlators in section 2.1.3 and which mostly are extensions of Slobodin's correlator[25].

Felstead[11] gives yet another form of a pseudo-coherent correlator: the squaring correlator, in which the correlation function:

$$P_{12}(\tau) = \int s_1^2(x)\, s_2^{\star 2}(x+\tau)\, dx \tag{3.1}$$

can be measured nearly in the same way as the linear correlation function, albeit that some bias removal technique must be applied here.

Especially for transmission mask type correlators the SNR and/or the dynamic range could be improved by the use of a laser[11,43].

4. A SIMPLE COHERENT OPTICAL CORRELATOR

4.1 Basic Principles

The correlator realized at our laboratory is of the spatial plane type with one transforming lens. In the output plane the squared correlation integral $|R_{12}(\tau)|^2$ is detected (see Section 2.1.1). Figure 2 gives schematically the experimental set up and the correlation detection.

The fixed reference function is a hard clipped phase plate, with essentially no zero order; the signal function is a photographic transparancy on which a biased modulated carrier wave is recorded.

Both transmission functions are put side-by-side directly in front of the transforming lens and are illuminated by a plane wavefront $A\, e^{j\omega t}$ from a HeNe laser.

To perform the correlation integral $|R_{12}(\tau)|^2$ intensity detection is applied in the frequency plane while moving the signal mask along the reference mask. The frequency axis is completely free from extraneous terms, but for one spectral term around the optical axis; however, correlation detection along with doppler shift indication, here also would be possible, since no zero-order peak is present. The complex transmission of the reference mask can be given by:

$$m(x) = e^{j\pi n_x} = +1 \text{ or } -1 \ . \tag{4.1}$$

Here n_x is the output of a 7-bits shift register and equals 0 or 1, so $m(x)$ is a pseudo-random hard clipped phase function.

If the signal function, to be correlated, is a modulated carrier wave $S_t(t)$:

$$S_t(t) = s(t) \cos 2\pi f_c t \tag{4.2}$$

and this function is recorded on a photographic transparancy as an amplitude transmission function $S_s(x)$, its transmission, when delayed by τ with respect to the reference mask, can be given by:

$$S_s(x+\tau) = a + bs(x+\tau)\cos 2\pi f_s(x+\tau) = \tag{4.3}$$

$$= a + \tfrac{1}{2}bs(x+\tau)e^{2\pi j f_s(x+\tau)} + \tfrac{1}{2}bs(x+\tau)e^{-2\pi j f_s(x+\tau)} \tag{4.4}$$

($f_c = f_s v$, v = film transport velocity).

The amplitude distribution in the focal plane of the Fourier lens is the Fourier transform of the product transmission of the two masks:

$$g(u\cdot\tau) = A\, e^{j\omega t}\cdot C\cdot e^{j\phi(u)}\int_{-D}^{+D} m(x)\, S_s(x+\tau)e^{-2\pi j(u/\lambda F)x}\,dx \tag{4.5}$$

the factor $e^{j\phi(u)}$ arises because the tranmission masks are not in the front focal plane of the transforming lens.

Substituting Equation (4.4) in Equation (4.5) we get three spectral terms which appear separated on the frequency axis for $f_s > W/2$; W = bandwidth of $m(x)$. After squaring we get in a region around $u = 0$ the intensity distribution:

$$I_0(u) = A^2C^2\left|\int_{-D}^{+D} a\, m(x)e^{-2\pi j(u/\lambda F)x}\,dx\right|^2 \tag{4.6}$$

and in $u = \lambda F f_s$ and in $u = -\lambda F f_s$:

$$I_{f_s}(\tau) = A^2C^2\left|\int_{-D}^{+D} \tfrac{1}{2}b\, m(x)\, s(x+\tau)\,dx\right|^2 . \tag{4.7}$$

Equation (4.7) gives the squared cross correlation function of $m(x)$ and $s(x)$: If $s(x) = m(x)$ (an ideal case of a received signal in an echo-doppler range system, that transmits $m(t)\cos 2\pi f_c t$) then Equation (4.7) transforms to the autocorrelation function of $m(x)$.

Since $m^2(x) \equiv 1$ this function will give δ-functions in $u = \pm\lambda F f_s$ for a delay $\tau = 0$ (due to the finite aperture the δ-functions become $|\sin\chi/\chi|^2$ functions).

In Figure 3 the intensity distribution is given for a delay $\tau = 0$ in correlating $m(x)$ with a nearly ideal signal film.

($s(x) = m(x)$, $a = b \approx \frac{1}{2}$). For $s(x) \equiv m(x)$ and the maximum value of $b = \frac{1}{2}$ it can be seen from (4.7) that the maximum attainable intensity in the correlation peaks is $(\frac{1}{2}b)^2 = \frac{1}{16}$ of the total intensity in the entrance aperture.

The intensity distribution around $u = 0$ arises from the constant a in $S_s(x+\tau)$ and gives Equation (4.6): the squared spatial frequency spectrum of the reference function $m(x)$.

In Figure 2 is shown schematically how the reference function is matched exactly with the modulation of the signal function at the moment of maximum correlation ($\tau = 0$).

At this moment the signal function will be demodulated and the generated carrier wave gives two δ-functions in the Fourier-plane, which are represented in Figure 3 by the correlation peaks at $f_s = 20$ lp/mm.

For a Δf_s doppler shifted signal ~~and~~ the Δf_s shifted carrier wave will be generated and the correlation peaks simply are displaced over Δf_s on the frequency axis. So range detection (from the time for which $\tau = 0$) and range-rate detection (from the shift on the frequency axis) can be performed simultaneously.

It will be shown that for a limited range of doppler shifts one and the same unshifted reference replica can be used.

The second dimension can be used then for processing several signals simultaneously.

4.2 Properties and Experimental Results

The Reference mask

The 127-element reference function $m(x)$ is realized as a hard clipped phase transmission function by supplying a quartz substrate with $\lambda/2$ layers in those regions where $m(x) = -1$.

By a combined evaporating and cutting technique the layers could accurately be constructed in any case to better than λ 25 , which is beyond the equivalent correlation detection accuracy. A single element was realized as a 10 mm line element of 0.1 mm width: so the spatial bandwidth is 10 lp/mm and the signal length is 12.7 mm. The compression ratio, that can be acquired with the function m(x) is equal to its time-bandwidth product, that is equal to 127. The peakwidth of the autocorrelation function then is expected to be 1/127 times the signal length, which is fully in agreement with the measured equivalent displacement $\tau = 0.1$ mm of the signal masks.

The signal masks

A number of photographic transparancies with biased 127-element coded carrier waves have been constructed according to Equation (4.3). The spatial carrier frequencies are varied from $f_s = 10$ lp/mm to $f_s = 20$ lp/mm with signal length variations of respectively -1% to $+1\%$.

In this way a range of doppler shifts Δf_c is simulated to $\Delta f_c = \pm 10^{-2} f_c$. Such a greatly enlarged fractional range of spatial frequencies with respect to the doppler shift range mostly can be produced for a real-time signal by mixing the received signal with a proper local oscillator frequency and recording the lower frequency component on a moving film (or applying to a ULM device if it concerns a signal in the μsec range).

According to Equation (4.7) the peakvalue of the squared correlation function is proportional to b^2 ; typical obtained values for the modulation depth b lie between 0.3 and 0.4 (for hard clipped computer plotted masks the maximum value $b = 0.5$ could be obtained).

The measured values of the correlation peaks agreed very well with the calculated ones, if the modulation depth b , the distance between the two masks and the signal length deviations are taken into account. When the two masks are not in the same plane, correlation with a Fresnel diffraction pattern of the reference mask will take place. The decrease of the correlation peaks due to this distance has been measured to be about 0.1 db/mm. In the experiments the distance between the masks was about 13 mm. The decrease of the peak values due to the signal length (= code length) deviations showed to be about 3 db for 1% length deviation[13].

For this purpose a series of signal masks has been constructed with all other parameters remaining constant, only the length was varied from 98% until 102% of the unshifted signal length (12.7 mm).

The results justify the use of one and the same unshifted reference function for a doppler shift range up to $\pm 1\%$, (moreover it is accurately defined where the lower values will appear on the frequency axis).

Resolving power

According to the Rayleigh criterium the number of resolved points on the frequency axis in a diffraction limited system are $D \cdot \Delta f_s = T \Delta f_c$ (= 127 for the above mentioned doppler series).
Here D = spatial signal length = entrance aperture of the system
Δf_s = spatial frequency range according to the doppler range of $\pm 1\%$
T = signal length (in sec)
Δf_c = carrier frequency range according to the doppler range of $\pm 1\%$

The equivalent range-rate range here is $\frac{\Delta f_c}{2 f_c} v = 10^{-2} v$, v = propagation velocity of the transmitted signal $S_t(t)$ in the relevant medium.

The resolution of the range-rate in general can be given by

$$\frac{\Delta f_c \cdot v}{2 f_c} / T \cdot \Delta f_c = v / 2 T f_c$$

and, for the above mentioned example by $10^{-2} v / D \cdot \Delta f_s = v/12700$, which gives for an acoustic signal transmitted in water a resolution of ~ 0.12 m/sec.

With a simple ($\sim$ 25 dollars) doublet of 900 mm focal length a decrease in resolution of about 10% of the diffraction limited values was obtained.

As mentioned before the width of the auto correlation function is 1/127 of the signal length and determines the resolution in range detection if the correlator is used in an echo-ranging system (e.g. an acoustic signal of 1.27 sec transmitted in water will give then a resolution in range detection of $1/2.1/100 \cdot v = 7.5$ m).

In a real-time moving film set-up the accuracy with which the film is transported from the recording stage to the correlation stage will become a critical parameter for the range resolution.

Film transport variations during the recording stage will give degraded correlation functions.

Ambiguity field

A reliable doppler shift detection will be possible only for signals which have no high cross-correlation terms in arbitrary points on the frequency axis. Therefore the whole (squared) ambiguity function $|g(u, \tau)|^2$ has been measured for an undistorted signal function (f_s = 15 lp/mm ; b = 0.38 ; 12.7 mm length).

With a photo-micrometer the squared cross-correlation functions have been measured in discrete points of the frequency axis from 10 lp/mm to 20 lp/mm: part of these measurements are given in Figure 4. The highest measured value in the field lies about 15 db and the averaged value in the field lies about 20 db below the value of the auto correlation peak that arises around f_s = 15 lp/mm and $\tau = 0$ (the envelope of the peaks along the frequency axis gives the diffraction due to the entrance aperture).

This is in agreement with the expected values: for an N-element function the averaged value in the ambiguity field is $1/\sqrt{N}$ of the auto-correlation peakvalue, and becomes $1/N$ for squared detection.

Application of typical system

The kind of signals that can be processed in the above described typical system depends on the type of signal recording that is applied.

In the experiments was thought of processing signals of rather long duration (e.g. 1 sec). Only non real-time photographic signal input was investigated.

For processing radarlike signals, which has not been investigated here, acousto-optical input devices can be applied[62]. The waveform that can be processed then, will depend on the properties of the applied U.L.M. device.

5. REAL-TIME OPERATION

5.1 Acousto-Optical Input Devices

The inherent two-dimensional nature of an optical system can give the optical signal processor an immense processing rate. By achieving this potential in real-time systems the optical computer probably can be competitive with other systems.

Realization however needs two-dimensional real-time input and output interface devices with adequate bandwidth and time-bandwidth products. One of the approaches could be the use of ultrasonic light modulators which as one-dimensional input devices are currently available[28,45].

The input signal is applied to a piezo-electric transducer, that launches an acoustic compressional wave (or shear wave) in a transparent liquid or solid medium. The travelling acoustic wave produces time varying fluctuations in the density and, hence, in the optical index of refraction, which appear to an impinging light beam as a moving spatial phase modulated pattern. The sound velocity in solids varies from $\sim 3.10^6$ mm/sec to $\sim 11.10^6$ mm/sec. The width of the needed optical wavefront, acoustic attenuation or the length of the available single crystals limit the length of the devices roughly to 30–100 mm and the range of signal lengths which can be processed to 0.2–20 μsec. This range makes the acousto-optical delay lines suitable for radar signal processors.

The acoustic attenuation limits the use of liquids to frequencies of about 20 MHz. Water for example shows an attenuation of 6 db/cm at 50 MHz (Ref.45): on the other hand it has a very high figure of merit for the diffraction efficiency. Isotropic solids are used up to ~150 MHz; fused silica is most popular, it has a very low attenuation (3 db/cm at 500 MHz) but also a relative low figure of merit; dense flint glasses and telluride glass show a far better figure of merit. This class, along with the lead molybdate devices, is the most important at the present time.

For high frequencies crystals must be used (alpha iodic acid and lead molybdate show a high figure of merit).

For the frequency range above 1GHz low loss materials such as rutile, sapphire, yag are used[46–48].

For different frequency ranges also different transducers are used. The use of piezo-ceramic materials is limited to 50–100 MHz because of their grain size. The use of single crystal materials like crystal quartz and lithium niobate is limited to 100–200 MHz because of bonding problems due to the thin slices. Evaporated transducers such as CdS and ZnO have been operated up to 10 GHz (Ref.48).

When the transducer works in the longitudinal mode the particle motion is in the same direction as the acoustic wave and gives rise to pure phase modulation: when the transducer works in the shear mode the particle motion is perpendicular to the acoustic wave propagation and gives rise to polarization modulation, which can be coverted to a pure amplitude modulation by inserting the device between crossed polarizers.

Types which show weak modulation generally work in the Raman-Nath mode and at frequencies below 50 MHz and types which show strong modulation generally work in the Bragg mode at frequencies above 150 MHz. In the intermediate region both types are possible; in fact, most of the commercially available acousto-optic devices (especially the deflectors) work in this frequency region and use Bragg reflection[49].

In Raman-Nath processors the optical wavefront is incident perpendicular to the acoustic wave propagation and the light rays travel through regions of homogeneous optical index of refraction which only is possible for acoustic beam diameters $1 \ll \Omega^2/4\lambda$, Ω = wavelength of acoustical wave, λ = wavelength of optical wave. This condition generally can be satisfied only for frequencies below about 50 MHz.

The phase excursion generally will be no larger than 0.2 radians which simplifies the generated pattern to the form given in Section 2.1.2. Most of the ULM devices used in the correlators of the cited references(Section 2.1) are of the Raman-Nath type and work at frequencies from 10 to 40 MHz, with time-bandwidth products from $TW = 10$ up to $TW = 100$.

{Some exceptions: Palfreeman[43] uses a special mirror imaging system to process signals up to 100 μsec ($TW = 1000$) and Gottlieb[50] uses acoustic path folding to process signals up to 1 msec ($TW = 10000$).}

Fused silica with crystal quartz transducers mostly are used in the class of Raman-Nath devices.

In general high time-bandwidth products only can be obtained at high frequencies: the condition $1 \ll \Omega^2/4\lambda$ will not be met then and the diffracted light rays no longer travel through regions of homogeneous index of refraction. Only for a rather small range of angles of incidence, for which the Bragg condition of reflection is satisfied, the diffracted rays will interfere constructively.

At this Bragg angle it is possible for a given acoustic power to diffract all the light in one single sideband. These Bragg-type devices mostly are used for processing linear FM radar signals[19,46] (see Section 2.3.2).

Time-bandwidth products up to $10^3 - 6.10^3$ have been achieved[28,46-48] in crystals of sapphire and rutile using CdS or ZnO transducers.

The frequency of the light, diffracted in acousto-optic devices, is shifted to an amount that is exactly equal to the applied acoustic frequency (for the first order diffracted beams).

This feature can also be used for signal processing by heterodyning the diffracted light with the undiffracted light[51].

Nowadays many firms are concerned with acousto-optic devices.

5.2 Film Type Input Devices

When film type input devices are used to perform real-time operation of an optical data processor in general only signals of relative long duration ($> 10^{-2}$ sec) can be processed.

For real-time operation the recording materials must need no development (or an instantaneous and short one) and must be erasable and reusable (a high write-erase cycle lifetime).

Furthermore for a practical device the materials should also show most of the features: high sensitivity, high resolution, a high read-out efficiency, a short recording time and sometimes a short erasure time.

The most important recording media are listed in Table 1 and a short description is given below.

Thermoplastic deformable media[5,52,53]

At the present time only thermo(photo)-plastic devices satisfy most of the listed requirements (see Table 1).

Thermoplastic film consists of a substrate coated with a thin transparent conducting layer which in turn is overlaid with a thin film of low melting temperature plastic.

If a surface charge pattern is recorded on the film and the film is heated to above its softening temperature then the film will deform in accordance with the recorded pattern. The pattern can be erased by heating the film above its melting temperature.

The surface charge pattern can be acquired by means of a scanning electron beam[10] or by a photoconductive layer, which is exposed to light according to the wanted pattern, while held under a constant electrostatic pressure.

After developing with a heat pulse which can be done nearly instantaneously and in situ, the recorded signal is acquired in the form of thickness modulation and acts as a spatial phase modulated pattern. Thermoplastic material responds only to a band of spatial frequencies which depends e.g. on the thickness of the thermoplastic layer. This frequency band response reduces intermodulation distortion[53].

Some firms or institutes which are concerned with thermoplastics are: CBS, RCA, GE, Radiation Inc., Bell Labs, University of Michigan.

Photochromics[5,57]

Photochromic materials change color spontaneously and reversibly when irradiated with light of a certain wavelength.

Typically in the bleached state they absorb radiation in the ultra violet and/or in the short wavelength region producing new absorption bands in the medium to the long-wavelength region of the visible spectrum. The types can be divided in organic, inorganic and glasses.

Photochromics need no development but unfortunately they show a very low sensitivity and decrease of sensitivity (fatigue) after some hundred write-erase cycles (except photochromic glass). Some firms which are concerned with photochromics are: American Cyanimid, Vari Light, Nuclear Research Ass., Corning, Carson Lab., RCA, Univac, IBM, NCR, ITEK, Thomson-Gobain, Zeiss.

Magneto-optics[5,52]

Certain ferromagnetic materials (in semi-transparent thin films) can be used for direct signal storage because of a different rotation of the plane of polarization produced by the different state of magnetization. Magnetic domains in the thin layer can be switched from one direction of magnetization to another by locally heating above its curie temperature (curiepoint writing) while it is under the influence of an opposite magnetic field.

Read-out can be accomplished by observing the polarization rotation in transmission (Faraday effect) or in reflection (Kerr effect). The disadvantages of these films are the very low diffraction efficiency and the requirement of very precisely controlled pulses of large amounts of power to perform the Curie-point writing. The most important material in this class is MnBi-film. Some firms concerned in this field are Honeywell, RCA (MnBi), IBM (EuO).

Ferro-electric photo-conductor devices[52,56]

With certain ferro-electric materials ferro-electric photo-conductor (FE-PC) devices can be made, which show optical recording and optical read-out possibilities.

The basic device consists of a ferro-electric slab (single crystal, ceramic or thin film) covered with a photo-conductive layer and sandwiched between transparent electrodes. Two typical state-of-the-art materials are $Bi_4 Ti_3 O_{12}$ and strain-biased PLZT.

Membrane light modulators[5]

The membrane light modulator, developed at Perking Elmer Co. is an optical spatial phase modulator which phase-modulates light reflected from its surface. The modulation is accomplished by electrostatic surface deformation of discrete surface elements.

As some less well-known or less developed recording materials can be mentioned: electro-optic materials, metal films, elastomer devices, liquid crystal photo-conductor devices, amorphous semi-conductor, acoustic surface waves.

Thermoplastic films with a relative good sensitivity (comparable to Kodak 649F plates), a high diffraction efficiency and a high cycle lifetime seems to date the most promising real-time reusable two-dimensional recording medium.

They are not yet commercially available, although several firms will have them ready for industrial implementation.

TABLE 1

Recording-device	*Ref.*	*Resolution* lp/mm	*Write energy* mJ/cm²	*Recording time* sec	*Write-erase cycle life-time*	*Read-out efficiency*	
Thermo-(photo) plastics	5	300	10^{-1}	10^{-8} (min.)	finite		erasure time 10 - 100 sec
	38		10^{-1}		many	> 10%	
	10	1000			10^{5}		erasure time < 1 sec
	54	1000	10^{-1} 4		> 100	7% 34%	
	53	4000	10^{-1}			40%	
	52	1000	10^{-3} (theor.)	10^{-3}	100	15%	erasure time 1 sec
Photo chromics	55	400	5.10^{3}	100	limited by fatigue		typical medium: KBR
	57	> 1000 > 2000	$10 - 10^{2}$ 10^{3}			3.7% 3.7%	inorganic materials KBR, glass, organic
	52	10,000	50	$\sim 10^{-9}$		1.2% - 3.7%	
Magneto-optics	52	1000	10	$10^{-11} \rightarrow 5.10^{-10}$		10^{-2}% (Faraday) 10^{-1}% (Kerr)	erase time ~1 μsec, MnBi
	55	400 100		10^{-6} 10^{-8}			MnBi EuO
M.I.M.	5	100	10^{-1}	10^{-8} (min.)	> 10^{12}		
Ferro-electric Photo-conductor devices	56	50	10	1	$10^{8} \rightarrow 10^{9}$		PLZT strain-biased
	52	800	1	10^{-3}	> 10^{5}	10^{-2}%	$Bi_4 Ti_3 O_{12}$
	52	50	10	1	limited by fatigue		PLZT strain-biased

6. CONCLUSIONS

Compared with electronic systems, optical analog techniques offer advantages in their large information capacity and inherent two-dimensional capability, allowing, for example simultaneous measurement of target range (time parameter) and range rate (spatial frequency) in any channel of a multi channel system.

An example is given in the described phase-plate-reference correlator in which only rather simple components are used and of which the results agree very well with the theoretical expectations. The experiments have been performed in a static laboratory set-up: hardly any parameter showed to be a critical one, but it is expected that in a real-time set-up the film transport velocity will be a critical parameter.

The kind of signals that can be processed in the described correlator depends on the type of signal recording that is applied.

The need of recording a (time) signal as an optical parameter generally is a disadvantage; especially for real-time operation sophisticated recording materials are necessary. A possible decrease of the dynamic range can be another disadvantage.

If the signal to be processed is available as a two-dimensional transmission picture and/or a typical operation such as a Fourier transform computation has to be performed, then the advantages of optical processing become quite obvious. Therefore the main application of optical computing to date have become the processing of synthetic aperture radar data and two-dimensional pattern recognition and image deblurring[6]. However, also much attention has been paid to digital picture processing[8,9,59,60].

It seems useful to make thorough comparisons between digital and optical techniques, including efficient processing speed and cost advantages.

Digital computers have a larger flexibility because they can be used also for non-linear operations and its accuracy can be far better than that of optical computers[8,9]. This latter however, can have a far larger processing speed, due to its two-dimensional parallel processing capability[6,8,9]. (10^{12} bits/sec have been achieved[5].) Coherent optical systems usually are cheaper than digital computers, however, this cannot simply be stated for all cases, or for future trends[8,9]. So, if a large number of calculations must be performed per unit time with only moderate accuracy the optical computer can be used to advantage. A continuous operation in real-time often will be required to make it fully advantageous.

Then suitable input and output interface devices are needed, which nowadays hardly are available.

For one-dimensional signals in the μsec range ultrasonic light modulators can ideally be used as real-time input devices. They are commercially available, but often their bandwidth and/or their diffraction efficiency is limited. Moreover only a limited number of channels can be handled simultaneously, which prevents real two-dimensional operation. The development of new high-efficient large-bandwidth transducers, for driving the ULM's, and of suitable solids and crystals with a high figure of merit and of course the development of two-dimensional acousto-optical devices, if possible, will still be very useful.

In order to construct really two-dimensional real-time input devices a number of reusable film types, of which thermo-plastic deformable film seems to be the most promising one, can be applied. It is expected that such films soon will be commercially available.

The coupling of digital and optical techniques to combine the advantages of both has had little attention up to now and the study of the possible applications may be useful[33].

The future trend of the efficient applicability of optical computing depends largely on the development of suitable input devices and of course on developments in alternative processing systems.

Electronic systems e.g. have the advantage that its fabrication largely can be automated which may result in a decrease in price. These techniques are not so easily applicable in the fabrication of optical systems.

Another alternative processing system possibly will be found in the application of acoustical surface wave devices[9,28,61].

7. REFERENCES

1. Lugt, A. vander — *Operational Notation for the Analysis and Synthesis of Optical Data-Processing Systems*. Proc. IEEE Vol.54, 9, 1055, September 1966.

2. Goodman, J.W. — *Introduction to Fourier Optics*. McGraw-Hill, 1968.

3. Shulman, A.R. — *Optical Data Processing*. John Wiley & Sons, Inc., 1970.

4. Papoulis, A. — *Systems and Transforms with Application in Optics*. McGraw-Hill, 1968.

5. Preston, K. Jr — *Coherent Optical Computers*. McGraw-Hill, 1972.

6. Stroke, G.W. — *Optical Computing*. IEEE, Spectrum Vol.9, 12, 24, December 1972.

7. Leith, E.N. — *Quasi-Holographic Techniques in the Microwave Region*. Proc. IEEE Vol.59, 9, 1305, September 1971.

8. Huang, T.S. et al. — *Image Processing*. Proc. IEEE Vol.59, 11, 1586, November 1971.

9. Preston, K. Jr — *A Comparison of Analog and Digital Techniques for Pattern Recognition*. Proc. IEEE Vol.60, 10, 1216, October 1972.

10. Doyle, R.J. — *Optical vs Digital Processing*. Laser Focus Vol.8, 10, 48, October 1972.

11. Felstead, E. — *Some Optical Correlators*. Research report No.70-2. Department of Electrical Engineering, Queen's University, Ontario, Canada, April 1970.

12. Jernigan, J.L. — *Correlation Techniques Using Microwaves*. Proc. IEEE Vol.56, 3, 374, March 1968.

13. Boden, J.A. — *A Simple Coherent Optical Correlator*. AGARD Conference Proceedings No.50, Paper 27, Tönsberg, 1969.

14. Felstead, E. — *A Simplified Coherent Optical Correlator*. Applied Optics Vol.7, 1, 105, January 1968.

15. Stark, H. et al. — *Optical Processing of Radar Signals with Fresnel Diffraction Masks*. Applied Optics Vol.10, 12, 2728, December 1971.

16. Di Tano, B. — *A More Flexible Optical Correlator Using Electro-Optical Doppler Replicas*. AGARD Conference Proceedings No.5, p.379, Paris, 1965.

17. Izzo, N.F. — *Optical Correlation Technique Using a Variable Reference Function*. Proc. IEEE Vol.53, 11, 1740, November 1965.

18. King, D.G. et al. — *Pulse Compression by Optical Correlation Techniques*. The Marconi Review Vol.XXXI, 171, 209, 1968.

19. Maloney, W.T. — *Acousto-Optical Approaches to Radar Signal Processing*. IEEE, Spectrum Vol.6, 10, 40, October 1969.

20. Atzeni, C. Pantani, L. — *A Simplified Optical Correlator for Radar-Signal Processing*. Proc. IEEE, Vol.57, 3, 344, March 1969.

21. Maloney, W.T. et al. — Comments on *A Simplified Optical Correlator for Radar-Signal Processing*. Proc. IEEE, Vol.57, 7, 1316, July 1969.

22. Atzeni, C. — *Optical Signal Processing by Filtering Fresnel Images of Acoustic Light Modulators*. Applied Optics Vol.11, 4, 863, April 1972.

23. Meltz, G. Maloney, W.T. — *Optical Correlation of Fresnel Images*. Applied Optics Vol.7, 10, 2091, October 1968.

24. Pantani, L. — *Some Experimental Confirmations of the Simplified Optical-Correlator Theory*. Proc. IEEE, Vol.60, 6, 750, June 1972.

25. Slobodin, L. — *Optical Correlation Technique*. Proc. IEEE Vol.51, 12, 1782, December 1963.

26. King, M. et al. — *Real-Time Electro-Optical Signal Processors with Coherent Detection*. Applied Optics Vol.6, 8, 1367, August 1967.

27. Atzeni, C. Pantani, L. — *Optical Signal-Processing through Dual-Channel Ultrasonic Light Modulators*. Proc. IEEE Vol.58, 3, 501, March 1970.

28. Squire, W.D. et al. — *Acousto-Optical Transversal Filters as Linear Signal Processors.* Proc. of the Techn. Programme Electro-Optics '71, p.153. Brighton 23–25 March 1971.

29. Aitken, G.J.M. Wang. L. — *New Multi Channel Optical Correlator.* Applied Optics Vol.10, 11, 2476, November 1971.

30. Felstead, E.B. — *Removal of the Zero Order in Optical Fourier Transformers.* Applied Optics Vol.10. 5, 1185, May 1971.

31. Lugt, A. vander — *Signal Detection by Complex Spatial Filtering.* IEEE Trans. IT-Vol.10, 2, 139, April 1964.

32. Lugt, A. vander — *A Review on Optical Data-Processing Techniques.* Optica Acta Vol.15, 1, 1, 1968.

33. Weaver, C.S. — *The Optical Convolution of Time Functions.* Applied Optics Vol.9, 7, 1672, July 1970.

34. Watrasiewicz, B.M. — *Optical Filtering.* Optics and Laser Technology Vol.4, 6, 288, December 1972.

35. Leith, E.N. — *Optical Processing Techniques for Simultaneous Pulse Compression and Beam Sharpening.* IEEE, AES-Vol.4, 6, 879, November 1968.

36. Brown, W.M. Porcello, L.J. — *An Introduction to Synthetic-Aperture Radar.* IEEE, Spectrum Vol.6, 9, 52, September 1969.

37. Larson, R.W. et al. — *A Microwave Hologram Radar System.* IEEE-AES-Vol.8, 2, 208, March 1972.

38. Lugt, A. vander — *Optical Processing.* Proceedings SPIE Vol.25, p.117. Developments in holography. Boston, April 1971.

39. Doyle, R.J. Glenn, W.E. — *Remote Real-Time Reconstruction of Holograms Using the Lumatron.* Appl. Opt. Vol.11, 5, 1261, May 1972.

40. Herman, St. — *Real-Time Electro-Optical Information Processors.* Electro-Technology Vol.79, 6, 52, June 1967.

41. Parks, J.K. — *Development of a Multi Channel Optical Correlation Detector for Sonar Signals.* J-Aircraft Vol.3, 3, 278, 1966.

42. Skenderoff, Cl. Pepin, Ch. — *Corrélation Optique pour Signaux Codés avec une Loi de Phase Pseudo-Aléatoire.* L'Onde Electrique, Vol.49, 8, 838, September 1969.

43. Palfreeman, J.S. — Een opto-akoestische correlator voor radardetectie. Philips Technisch Tijdschrift Vol.28, 8/9/10, 318, 1967.

44. Talamini, A.J. Farnett, E.C. — *New Target for Radar: Sharper Vision with Optics.* Electronics Vol.38, 26, 58, 1965.

45. Adler, R. — *Interaction between Light and Sound.* IEEE Spectrum Vol.4, 5, 42, May 1967.

46. McMahon, D.H. — *Wide-Band Pulse Compression via Brillouin Scattering in the Bragg Limit.* Proc., IEEE Vol.55, 9, 1602, September 1967.

47. Flinchbauch, D.E. — *Acousto-Optic Laser Modulation.* Laser Focus Vol.3, 11, 25, September 1967.

48. King, D.G. — *Ultrasonic Delay Lines for Frequencies above 100 MHz.* The Marconi Review, Vol.XXXIV, 183, 314, fourth quarter 1971.

49. Alphonse, G.A. — *Broad-Band Acousto-Optic Deflectors Using Sonic Gratings for First-Order Beam Steering.* RCA Review, Vol.33, 3, 543, September 1972.

50. Gottlieb, M. et al. — *Opto-Acoustic Processing of Large Time-Bandwidth Signals.* Applied Optics Vol.11, 5, 1069, May 1972.

51. Brienza, H.J. Heynau, H.A. — *Laser-Acoustic Signal Processing.* AGARD Conference Proceedings No.50. Paper 30, Tönsberg 1969.

52. Bordogna, J. et al. — *Recyclable Holographic Media*. RCA Review, Vol.33, 1, 227, March 1972.

53. Credelle, T.L. Spong, F.W. — *Thermoplastic Media for Holographic Recording*. RCA Review, Vol.33, 1, 206, March 1972.

54. Norman, S.L. — *Holography in Unconventional Materials*. Optical Spectra, Vol.4, 10, 26, November 1970.

55. Chen, D. Tufte, O.N. — *Optical Memories. Now and in the Future*. Electronics World, Vol.84, 4, 56, October 1970.

56. Maldonado, J.R. Meitzler, A.H. — *Strain-Biased Ferro-Electric Photo-Conductor Image Storage and Display Devices*. Proc. IEEE, Vol.59, 3, 368, March 1971.

57. Pressley, R.J. — *Handbook of Lasers*. Ed. Robert J.Pressley. Ph.D. The Chemical Rubber Co, Ohio, 1971.

58. Jenney, J.A. — *Holographic Recording with Photo-Polymers*. J.O.S.A., Vol.60, 9, 1155, September 1970.

59. — — *Special Issue on Digital Picture Processing*. Proc. IEEE, Vol.60, 7, July 1972.

60. Andrews, H.C. Pratt, W.K. — *Digital Computer Simulation of Coherent Optical Processing Operations*. Computer Group News, Vol.2, 6, 12, November 1968.

61. Quate, C.F. Thomson, R.B. — *Convolution and Correlation in Real-Time with Non-Linear Acoustics*. Appl. Phys. Lttrs, Vol.16, 12, 494, 15 June 1970.

62. Skenderoff, C. — *Traitement des Signaux Radars par Correlation Optique*. AGARD Conference Proceedings No.50, Paper 28, Tönsberg 1969.

63. Takai, N. — *A Unified Treatment of Real-Time ULM Correlators*. Opto-Electronics, Vol.5, 5, 393, September 1973.

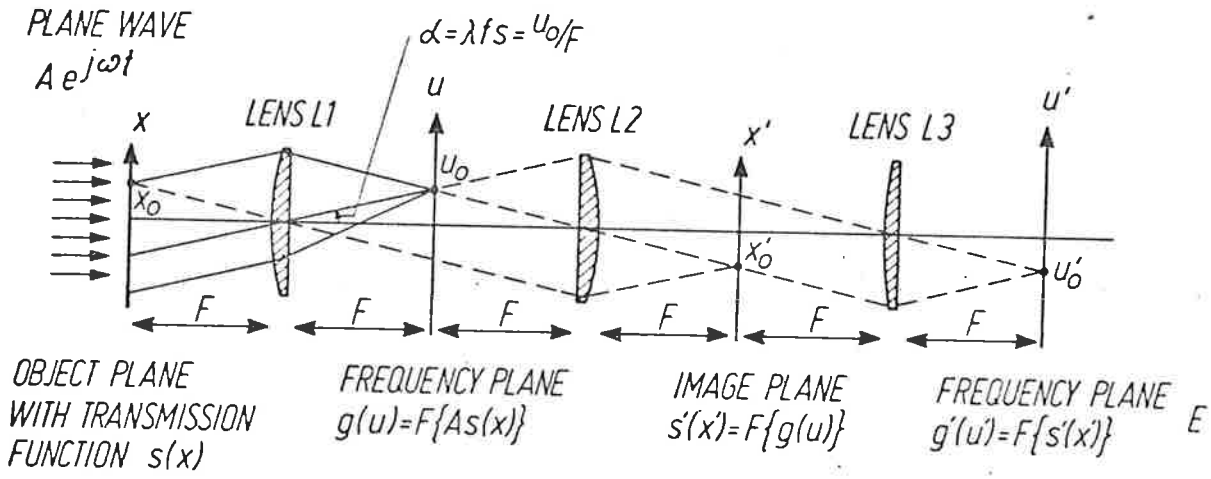

Fig.1 Basic configuration of optical data processing system

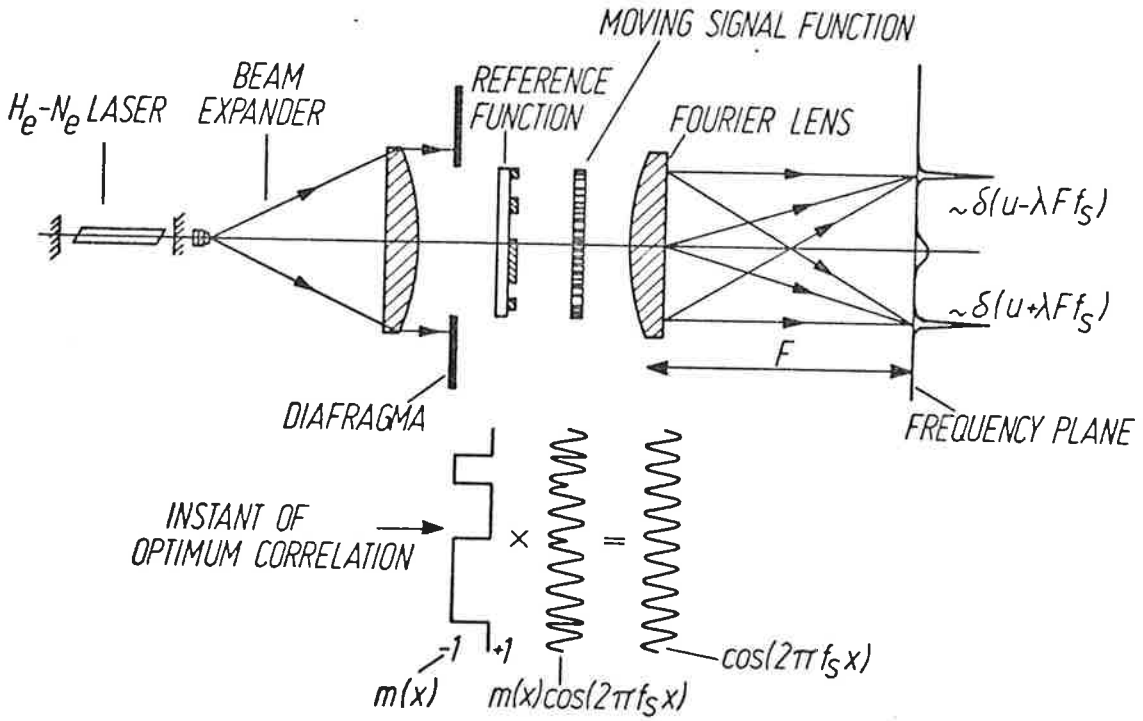

Fig.2 Schematic of the simple optical correlator; the lower part gives schematically the ideal correlation of a modulated carrier wave with its modulation function

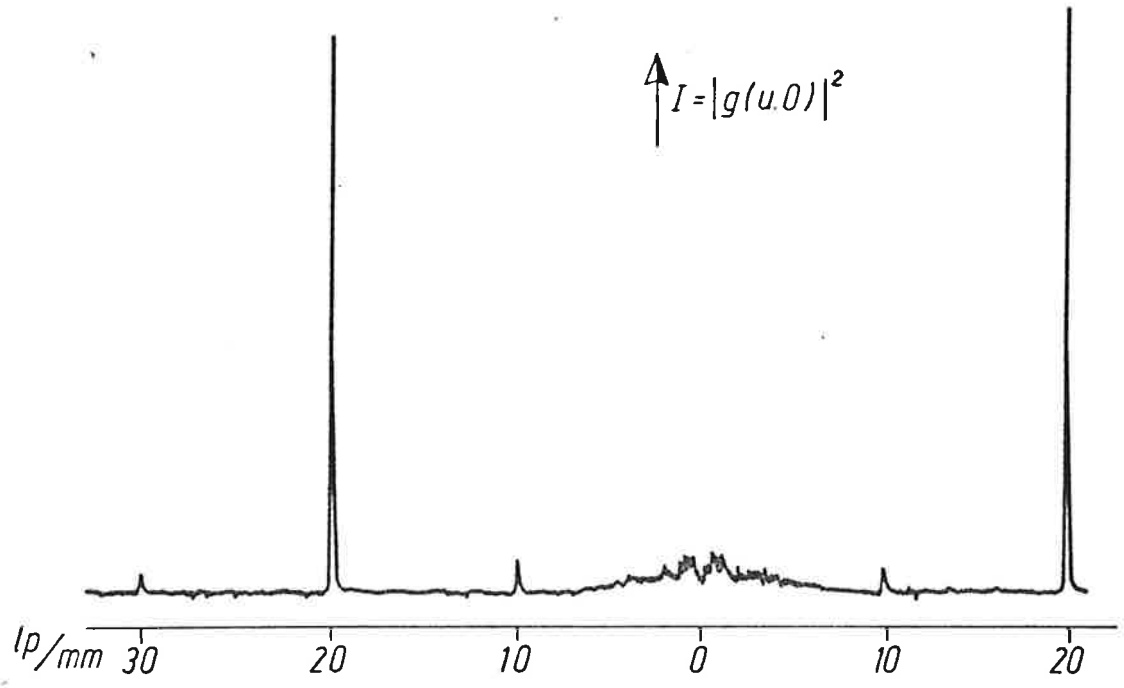

Fig.3 Intensity distribution on the spatial frequency axis at the moment of optimum correlation (carrier frequency of the correlated signal function is 20 lp/mm)

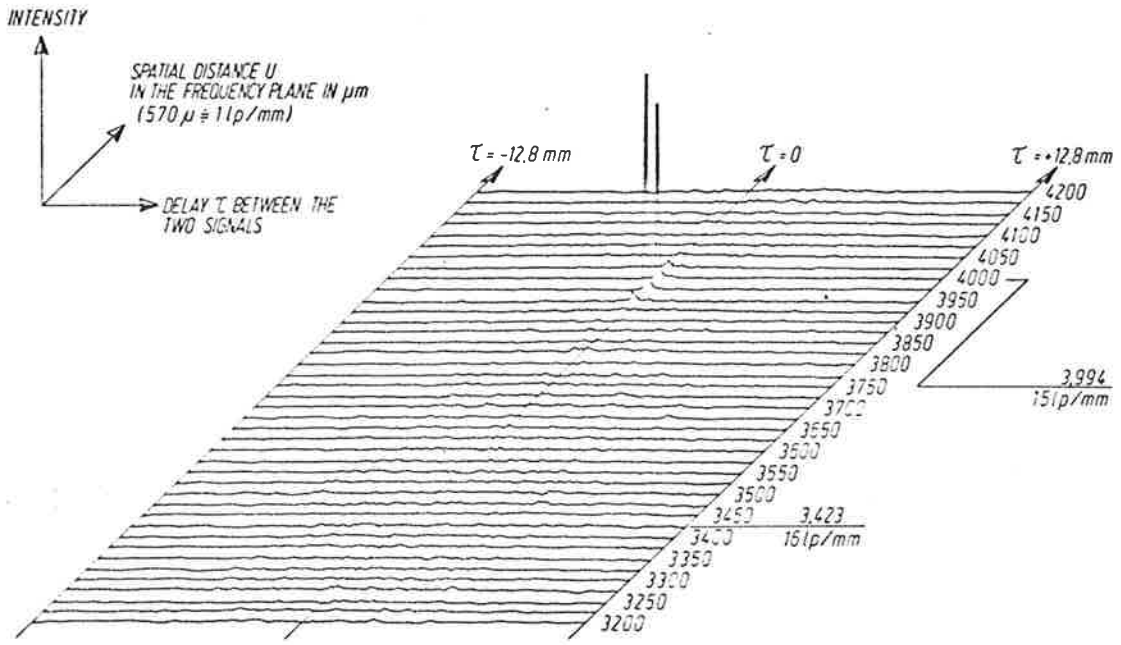

Fig.4 Part of the (squared) ambiguity function around one of the two correlation peaks (carrier frequency of the correlated signal function is 15 lp/mm)